Modelling the effects of temperature-dependent material properties in shear melt layers

Robert Timms and Richard Purvis

School of Mathematics, University of East Anglia,
Norwich, NR4 7TJ, United Kingdom
r.timms@uea.ac.uk

Abstract: The mechanisms responsible for ignition of explosive materials in response to low energy stimuli, known as "insults" in the literature, are still not well understood. It is in general believed that explosive ignition is of thermal origin, with mechanical energy being converted into heat energy in localised regions, forming so-called "hot spots". When an explosive sample is subject to a mechanical insult pre-existing, or new, microcracks will be in compression and shear. It is possible for such microcracks to grow in size if the local stress is great enough and, due to friction between solid surfaces, heat is released during the growth process. Subsequent to sufficient heat release, the crack surface temperature will be raised to the solid melting point and a thin sheared melt layer will be formed, separating the solid surfaces. This thin melt layer will continue to be heated through viscous dissipation and subsequent chemical reaction, and is thought to be a prime location for so-called hot spot generation.

Mechanical insults, resulting from low-speed impacts which shear an explosive, have been identified as a possible ignition source. However, modelling such an ignition mechanism numerically with hydrocodes proves to offer some considerable challenges. To supplement the numerical approach, we develop an analytical model of the shearing, melting and subsequent ignition of an explosive material. We consider the melting of a thin viscous layer of explosive material due to an applied shear in an idealised planar geometry. The model accounts for self-heating due to mechanical dissipation, and a single-step Arrhenius reaction is used to describe the heating of the explosive due to subsequent chemical reaction. A solution is sought by considering perturbations from a melt layer of uniform width. In particular, we consider the effects of modelling the temperature dependence of the liquid viscosity and specific heat are studied. In contrast to previous work which does not account for the temperature dependence of material properties, it is shown that allowing the viscosity to vary with temperature can lead to non-uniform mechanical heating in the layer to leading order. Such localised heating may be associated with generation of localised hot spots which give rise to ignition.

1 Introduction

Mechanical insults, resulting from low-speed impacts which shear an explosive, have long been identified as a possible ignition source in reactive materials. In particular, it is possible for thin molten layers of explosive material to form within an explosive sample as a result of shear. In this paper we present a model describing the heating of thin molten layers of explosive material undergoing shear. The model was originally formulated to investigate the possibility of local material inhomogeneity being a mechanism for hot spot formation and subsequent thermal runaway. Here we investigate further to see if allowing the material properties to be a function of temperature can give rise to new hot spot mechanisms, or affect the behaviour of the mechanisms observed when modelling shear melt layers with constant material properties. Ultimately, improved understanding of the mechanisms which have the capability to induce localised temperature increase will aid in the design of safe storage and handling procedures for explosive materials.

Numerous mechanisms arising from shear are widely discussed in the literature. For instance, Bowden et al. [5], Ubbelohde [18], Bowden and Gurton [3], and Bowden and Yoffe [4] all discuss frictional rubbing as a well established ignition mechanism. During rubbing contact between two solids, the hot spot temperature is determined by the solid with the lower melting point – the lower melting point solid 'quenches' the hot spot temperature to the melting temperature. Bowden and Gurton were able to measure hot spot ignition temperatures for a wide range of explosives by choosing grits of different melting points and measuring the effect on the sensitivities of the explosives [3].

Shear localisation has been widely studied in inert materials, see, for example, Bai and Dodd [?], and DiLellio and Olmstead [10]. There have been very few analytical studies on localised shear in explosive materials. However, many experimental studies can be found in the literature. Evidence for localised shear within the explosive sample can be observed in recovered unexploded samples. Photographic evidence for adiabatic shear is given by Field et al. [11], showing ignition and propagation occurring in a shear band in a sample of PETN (pentaerythritol tetranitrate). Notable work on shear localisation in explosive materials includes: Boyle et al. [6]; Chen et al. [7]; Dienes [9]; Frey [12]; and the substantial work by Afanas'ev and Bobolev [1]. Also worthy of mention are the experimental works by Howe et al. [13] and Mohan et al. [15]. It is in general concluded that localised shear is a prevalent hot spot mechanism, which manifests in many differing loading scenarios.

Investigation of these effects through the use of numerical continuum mechanics methods, such as finite element models, often breaks down owing to problems such as severe mesh deformation [8]. Typically, a very high resolution is required to overcome these issues, but this comes at the cost of computational resources and time. Additionally, large scale numerical codes do not always offer as much physical insight as small scale, simplified, analytical models. Such simplified models are to be employed here to try and gain a deeper understanding of the mechanisms which lead to thermal

runaway.

Starobin and Dienes [16] present a one-dimensional model for the lateral melting and ignition of a thin sheared viscous layer. In their work a self-similar solution for parabolic melt front propagation in non-reactive materials is found, as well numerical results for non-steady sliding of the crack surface and a non-linear Arrhenius source term. The results presented demonstrate that shear melting in the one-dimensional geometry leads to an increase in the peak hot spot temperature relative to the melting point of HMX (cyclotetramethylene tetranitramine). Recently, this model was formally derived and extended into two spatial dimensions [17].

In their study, Starobin and Dienes [16] treat all material properties as constant, allowing one to reasonably assume a linear velocity profile across the melt layer. However, the temperature across the layer varies from the melt temperature of $520\,\mathrm{K}$ to a peak temperature of over $700\,\mathrm{K}$. Inevitably this large increase in temperature will have some effect on the material properties. In particular, it is suggested that the viscosity may vary significantly across the layer, and the linearisation of the fluid velocity across the layer would break down.

Here we further the develop the two-dimensional model, allowing the specific heat and viscosity to vary with temperature. We introduce temperature-dependent specific heat by means of an Einstein relation, as used in the numerical simulation for shear localisation presented by Austin et al. [2], and the viscosity of the liquid phase of HMX is modelled using an Arrhenius law, which accounts for the dependence of the viscosity on temperature. The thinness of the melt layer is exploited, and a lubrication analysis is made. Within the lubrication approximation, small deviations from the one-dimensional solution are considered and an asymptotic solution is calculated numerically up to first order.

2 Mathematical Model

We consider a semi-infinite solid block of explosive material occupying the region $x > 0$, with a rigid wall located at $x = 0$, where x is the horizontal coordinate in the usual Cartesian coordinate system. At time $t = 0$ the wall moves impulsively downwards with speed v_w. The movement provides a shear force on the explosive sample, generating sufficient heat to melt the material near the wall, such that at $t = t_0$ there already exists a thin viscous liquid melt layer adjacent to the wall, see Figure 1.

The problem formulation is as in [17], where the non-dimensional variables are: the velocity components in the melt layer (u, v) in the (x, y) directions, the pressure p, and temperature T. Note, all variables have been non-dimensionalised using the wall speed v_w, time scale t^*, density ρ, reference specific heat c^*, reference viscosity μ^* and temperature difference ΔT. The reference values for the material properties may be found in Table 1. Currently the time scale t^* is chosen to give a correct order of magnitude for the time to thermal runaway when compared with results from experiments. However, further work could be undertaken to calibrate the time scale, thus giving
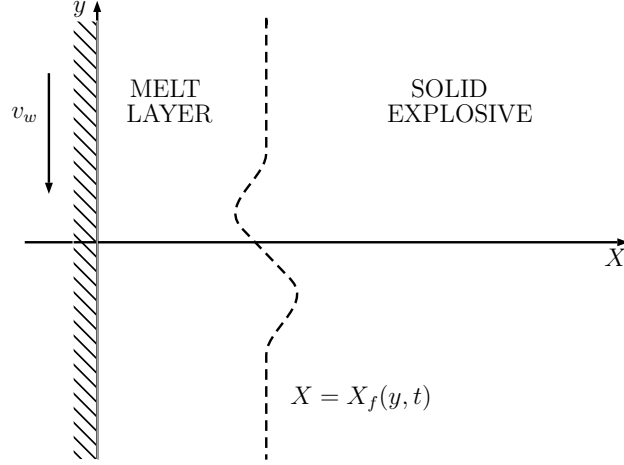
3

Figure 1: Shear melt layer model.

more accurate predictions for the time to runaway.

The explosive sample is initially heated by viscous dissipation in the melt layer and, once the temperature rise is sufficient, heated further by a consequent chemical reaction. As in previous work, e.g. Curtis [8], this is modelled using a single step Arrhenius reaction

$$\frac{\partial \alpha}{\partial t} = \hat{A}(1 - \alpha)\exp\left(-\frac{\hat{E}}{T}\right), \tag{1}$$

where $\hat{A} = t^* A$ is the non-dimensional pre-exponential factor, $\hat{E} = E/(R\,\Delta T)$ is the non-dimensional activation energy, E is the activation energy, R is the molar gas constant and α the mass fraction, ranging from 0 (unreacted) to 1 (fully reacted). The conservation of energy equation thus reads

$$c(T)\frac{\mathrm{D}T}{\mathrm{D}t} = \frac{1}{\mathrm{Pe}}\nabla^2 T + \frac{\mathrm{Ec}\,\mathrm{Pr}}{\mathrm{Pe}}\Phi + \hat{\Omega}\frac{\partial \alpha}{\partial t}, \tag{2}$$

where $\mathrm{Pe} = (c^*\rho v_w^2 t^*)/\kappa$ is the Péclet number, $\mathrm{Ec} = v_w^2/(c^*\Delta T)$ is the Eckert number, $\mathrm{Pr} = (c^*\mu^*)/\kappa$ is the Prandtl number, κ is the thermal conductivity, and $\hat{\Omega} = \Omega/(c^*\Delta T)$ is the non-dimensional heat of reaction, where Ω is the specific heat of the reaction. The viscous dissipation in the melt layer is given by

$$\Phi = 2\mu\left[\left(\frac{\partial u}{\partial x}\right)^2 + \left(\frac{\partial v}{\partial y}\right)^2 - \frac{1}{3}\left(\frac{\partial u}{\partial x} + \frac{\partial v}{\partial y}\right)^2\right] + \mu\left(\frac{\partial v}{\partial x} + \frac{\partial u}{\partial y}\right)^2. \tag{3}$$

The relation between the (dimensionless) specific heat c and temperature is given by

$$c(T) = \frac{(\theta_1/T)^2 \exp(\theta_1/T)}{(\exp(\theta_1/T) - 1)^2}, \tag{4}$$

4

where $\theta_1 = (1000\,\mathrm{K})/\Delta T$. This particular functional form has been used by Austin et al. [2] to describe the heat capacity for the β phase of HMX, and it is therein assumed that the heat capacity of the liquid phase is identical to that of the solid phase. In the interest of simplicity we make the same assumption here and use the above relation for the specific heat of liquid HMX. The temperature dependence of the viscosity μ is modelled using an Arrhenius law

$$\mu(T) = \exp\left(\frac{\theta_2}{T} - \frac{\theta_2}{\theta_3}\right), \tag{5}$$

where $\theta_2 = (7800\,\mathrm{K})/\Delta T$ and $\theta_3 = (800\,\mathrm{K})/\Delta T$ are experimentally determined constants.

The non-dimensional specific heat and viscosity are related to their dimensional counterparts through the scalings $c^* = 1034\,\mathrm{J\,kg^{-1}\,K^{-1}}$ and $\mu^* = 5.5 \times 10^{-3}\,\mathrm{kg\,m^{-1}\,s^{-1}}$, respectively. For the viscosity we use the values given by Menikoff and Sewell [14], who state that at $800\,\mathrm{K}$ the viscosity of HMX drops to $5.5 \times 10^{-3}\,\mathrm{kg\,m^{-1}\,s^{-1}}$, whereas the scaling for the specific heat has been chosen to compare well with previous modelling.

The dynamics of the liquid layer are governed by the Navier-Stokes equations. In previous work which developed a model of a shear melt layer with constant material properties it was shown that a lubrication approximation is appropriate, due to the assumed thinness of the melt layer [17]. To account for this thinness, we adopt the following scalings in the liquid region

$$x = \varepsilon X, \quad u = \varepsilon U, \quad p = \varepsilon^{-2} P, \tag{6}$$

where $\varepsilon = \mathrm{Pe}^{-1/2}$. These scalings are substituted into the Navier-Stokes equations and only the leading order terms are retained. The resulting governing equations of motion are the lubrication equations

$$\frac{\partial U}{\partial X} + \frac{\partial v}{\partial y} = 0, \tag{7}$$

$$\frac{\partial P}{\partial X} = 0, \tag{8}$$

$$-\frac{\partial P}{\partial y} + \frac{\partial}{\partial X}\left(\mu(T)\frac{\partial v}{\partial X}\right) = 0, \tag{9}$$

which are based on the usual assumption that both $\varepsilon \ll 1$ and $\varepsilon^2 \, \mathrm{Re} \ll 1$. The equations $(7) - (9)$ are to be solved subject to no-slip boundary conditions on the wall $X = 0$ and melt front $X = X_f$, that is

$$U = 0, \qquad v = -1 \qquad \text{on } X = 0, \tag{10}$$

$$U = 0, \qquad v = 0 \qquad \text{on } X = X_f. \tag{11}$$

We expect that far from the site of the the two dimensional disturbance that the solution will

Explosive Property	HMX
Activation Energy E	$2.2 \times 10^5 \, \text{J mol}^{-1}$
Heat of Reaction Ω	$5.02 \times 10^6 \, \text{J kg}^{-1}$
Molar Gas Constant R	$8.314 \, \text{J kg}^{-1} \, \text{K}^{-1}$
Pre-Exponential Const. A	$5.011\,872\,336 \times 10^{19} \, \text{s}^{-1}$
Density ρ	$1860 \, \text{kg m}^{-3}$
Reference Viscosity μ^*	$5.5 \times 10^{-3} \, \text{kg m}^{-1} \, \text{s}^{-1}$
Latent Heat L	$2.08 \times 10^5 \, \text{J kg}^{-1}$
Melting Temperature T_m	$520.6 \, \text{K}$
Reference Specific Heat c^*	$1034 \, \text{J kg}^{-1} \, \text{K}^{-1}$
Thermal Conductivity κ	$0.404 \, \text{W m}^{-1} \, \text{K}^{-1}$

Table 1: Material properties for HMX taken from Curtis [8], Menikoff and Sewell [14] and Starobin and Dienes [16].

resemble the one dimensional solution, and that the pressure will be constant. It is sufficient to impose the following condition on the pressure

$$\frac{\partial P}{\partial y} \to 0 \quad \text{as } y \to \pm\infty. \tag{12}$$

After substitution of the scalings (6), the energy equation (13) reads

$$c(T)\frac{\mathrm{D}T}{\mathrm{D}t} = \frac{\partial^2 T}{\partial X^2} + \mathrm{Ec}\,\mathrm{Pr}\,\Phi + \hat{\Omega}\frac{\partial \alpha}{\partial t}, \tag{13}$$

where $\Phi = \mu(T)(\partial v/\partial X)^2$. The energy equation (13) is to be solved subject to the following boundary conditions on the temperature

$$\frac{\partial T}{\partial X} = 0 \qquad \text{at } X = 0, \qquad\qquad T = T_m \qquad \text{at } X = X_f(y,t), \tag{14}$$

$$\frac{\partial T}{\partial y} \to 0 \qquad \text{as } y \to \infty \qquad\qquad \frac{\partial T}{\partial y} \to 0 \qquad \text{as } y \to -\infty, \tag{15}$$

where T_m is the non-dimensional melting temperature. The location of the melt front X_f is determined by the Stefan condition, which equates the temperature flux discontinuity with the magnitude of the latent heat sink at the phase boundary

$$\frac{\partial X_f}{\partial t} = -\mathrm{Ste}\left.\frac{\partial T}{\partial X}\right|_{X=X_f^-}, \tag{16}$$

where $\mathrm{Ste} = (c^*\Delta T)/L$ is the Stefan number, which is the ratio of sensible heat to latent heat, L. The initial melt front is a prescribed function of y, written $X_f(y,t_0)$, and is allowed to evolve in time.

2.1 Perturbation scheme

In this section we consider small deviations from a uniform-width melt front $X_f = X_f(t)$ by means of the small parameter $\delta \ll 1$ which characterises the size of the two-dimensional disturbance. We look for a solution in terms of a perturbation series in, i.e.

$$(X_f, P)(y, t) = (X_{f0}, P_0)(t) + \delta(X_{f1}, P_1)(y, t) + O(\delta^2), \tag{17}$$

$$(U, v, T, \alpha)(\xi, y, t) = (U_0, v_0, T_0, \alpha_0)(\xi, t) + \delta(U_1, v_1, T_1, \alpha_1)(\xi, y, t) + O(\delta^2), \tag{18}$$

$$(c, \mu)(\xi, y, t) = (c_0, \mu_0)(\xi, t) + \delta(c_1, \mu_1)(\xi, y, t) + O(\delta^2), \tag{19}$$

where we have introduced the front-fixed coordinate $\xi = X/X_{f0}$ which fixes the melt front at $\xi = 1$ to leading order, and later proves useful in numerical computations. In order to introduce two-dimensional effects into the model we impose a shape on the initial melt front, which must decay to the corresponding one-dimensional melt width at the infinity. It is recognised that the specific heat and viscosity may be expressed in terms of the temperature expansion. However, their expansions provide a useful notational convenience. These expansions may be substituted into the governing equations, and collecting terms with like powers of δ forms a hierarchy of problems which may be solved numerically.

Since the viscosity is temperature-dependent, the momentum and energy equations do not decouple, as is typically the case in lubrication theory. However, we may obtain the following expression for the leading order vertical velocity component

$$v_0(\xi, t) = \left(\int_0^1 \frac{1}{\mu_0} \, d\xi \right)^{-1} \int_0^\xi \frac{1}{\mu_0} \, d\xi - 1. \tag{20}$$

Obtaining the first order correction requires a little more work. However, the problem is somewhat simplified if we assume that the first order correction have a particular y dependence. By virtue of the lubrication equations, the first order corrections have the following form

$$X_{f1} \sim X_{f1}(t) S(y), \quad U_1 \sim U_1(\xi, t) S'(y), \quad v_1 \sim v_1(\xi, t) S(y), \quad \frac{\partial P_1}{\partial y} \sim P_1(t) S(y),$$

$$T_1 \sim T_1(\xi, t) S(y), \quad \alpha_1 \sim \alpha_1(\xi, t) S(y), \quad c_1 \sim c_1(\xi, t) S(y), \quad \mu_1 \sim \mu_1(t) S(y), \tag{21}$$

where the shape function $S(y)$ gives the y dependence of the melt front location. As a first approximation, derivatives of the shape function are neglected. This may place some restriction on the choice of initial melt front shape $X_f(y, t_0)$. However, full numerical simulations of the shear melt model with constant material properties reveal that the magnitude of the horizontal velocity component is indeed small for the initial melt front shapes used in this study.

Substitution of the expansions (17) – (19) into the governing equations (7) – (16), and collecting terms $O(\delta)$ gives an expression involving the first order velocity correction, which may be integrated

twice to obtain

$$v_1(\xi,t) = X_{f0}^2 P_1 \int_0^\xi \frac{\xi'}{\mu_0}\,\mathrm{d}\xi' - \int_0^\xi \frac{\mu_1}{\mu_0}\frac{\partial v_0}{\partial \xi'}\,\mathrm{d}\xi' + d_1(t)\int_0^\xi \frac{1}{\mu_0}\,\mathrm{d}\xi' + d_2(t). \tag{22}$$

Application of the boundary conditions gives

$$d_1(t) = -\left(\int_0^1 \frac{1}{\mu_0}\,\mathrm{d}\xi'\right)^{-1}\left[\frac{X_{f1}}{X_{f0}}\left.\frac{\partial v_0}{\partial \xi}\right|_{\xi=1} + X_{f0}^2 P_1 \int_0^1 \frac{\xi'}{\mu_0}\,\mathrm{d}\xi' - \int_0^1 \frac{\mu_1}{\mu_0}\frac{\partial v_0}{\partial \xi'}\,\mathrm{d}\xi'\right], \tag{23}$$

$$d_2(t) = 0. \tag{24}$$

Integration of the continuity equation across the gap width provides the first order pressure correction

$$P_1(t) = \frac{1}{X_{f0}^2}\frac{\int_0^1\left(\int_0^{\xi'}\frac{\mu_1}{\mu_0}\frac{\partial v_0}{\partial \xi''}\,\mathrm{d}\xi'' + \frac{\int_0^{\xi'}\frac{1}{\mu_0}\,\mathrm{d}\xi'}{\int_0^1\frac{1}{\mu_0}\,\mathrm{d}\xi'}\left[\frac{X_{f1}}{X_{f0}}\left.\frac{\partial v_0}{\partial \xi}\right|_{\xi=1} - \int_0^1\frac{\mu_1}{\mu_0}\frac{\partial v_0}{\partial \xi''}\,\mathrm{d}\xi''\right]\right)\mathrm{d}\xi'}{\int_0^1\left(\int_0^{\xi'}\frac{\xi''}{\mu_0}\,\mathrm{d}\xi'' - \frac{\int_0^{\xi'}\frac{1}{\mu_0}\,\mathrm{d}\xi'}{\int_0^1\frac{1}{\mu_0}\,\mathrm{d}\xi'}\int_0^1\frac{\xi''}{\mu_0}\,\mathrm{d}\xi''\right)\mathrm{d}\xi'} \tag{25}$$

The vertical velocity components (20) and (22) may then be substituted into the energy equation, reducing the problem to a set of two coupled partial differential equations (PDEs) – one for the temperature and another for the reaction extent. The resulting PDEs are solved numerically using an iterative Crank-Nicolson scheme.

3   Numerical Results

Results are given for a sample of HMX subject to a uniform wall speed $v_w = 70\,\mathrm{m\,s^{-1}}$. See Table 1 for material properties of HMX. It is assumed that at time $t = t_0$ a melt layer has already been formed. In previous work, an early-time solution has been found which provides an initial condition for the simulation [17]. When studying a non-uniform melt layer two-dimensional effects are introduced via an imposed shape function, giving initial melt front $X_f(y, t_0)$. Such effects may manifest physically as a result of the inhomogeneous nature of the explosive material. For example, material properties may locally differ in space, causing some areas to melt more rapidly than others, thus resulting in a non-uniform melt width. The aim of this work is not to describe how such two-dimensionality may arise, but to study the effects spatial variations in the melt front may have on the temperature field and time to runaway.

In Section 3.1 we present the leading order solutions, demonstrating a departure from the linearised velocity profile assumed by Starobin and Dienes [16] and the resulting localisation in the mechanical heating across the layer. Note that the leading order problem is the temperature-dependent material properties analogue of the model presented by Starobin and Dienes [16]. We

then present an example two-dimensional solution in Section 3.2, which is computed up to $O(\delta)$ in the perturbation scheme. It is shown that the localisation mechanisms that arise due to the melt front disturbance persist when we relax the assumption of constant specific heat and viscosity. In the interest of brevity we only present a single two-dimensional solution to illustrate the effects of temperature-dependent material properties, but similar conclusions hold for the other melt front shapes discussed in previous work [17].

3.1   One-dimensional results

Figure 2 shows the leading order specific heat and viscosity across the melt layer at a series of increasing times. We observe that the specific heat increases with temperature, with the shape of the plot looking much like a typical temperature profile across the layer (compare with Figure 4). Conversely, the viscosity decreases with temperature and thus takes its smallest value adjacent to the moving wall where the temperature is greatest. Interestingly we see very little change in the viscosity as a function of time, with all snapshots virtually coinciding. The initial temperature profile is such that we already observe a dramatic decrease in the viscosity across the melt layer, and the local changes in temperature have relatively little effect on the viscosity as time proceeds.
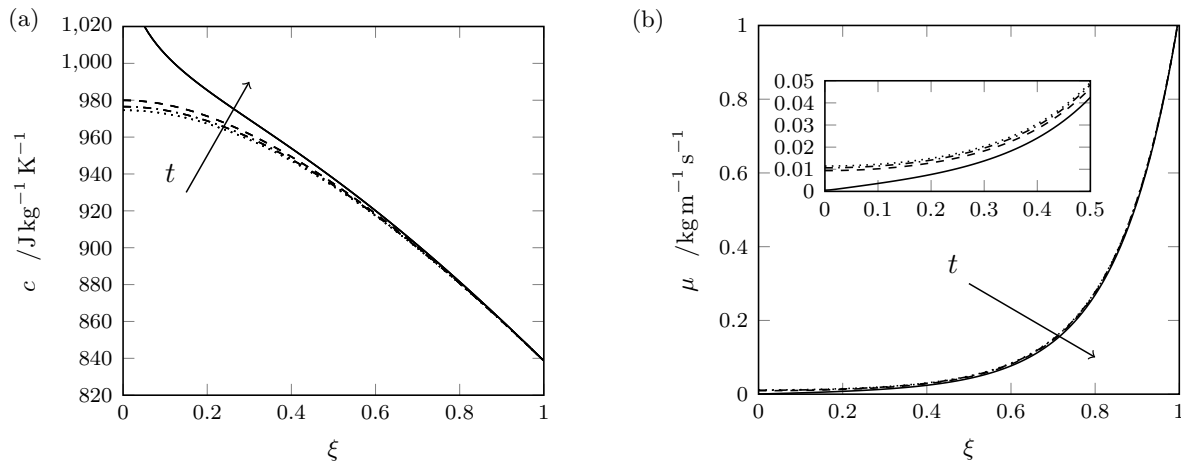

Figure 2: (a) The dimensional specific heat c across the melt layer at times $t = 501, 992, 1483$ and $1974 \, \mathrm{ns}$. (b) The dimensional viscosity μ across the melt layer shown at the same times.

Figure 3 shows the leading order vertical velocity and mechanical dissipation across the melt layer. As predicted by Starobin and Dienes [16], most of the slip is supported by the melt layer near the sliding surface, and the velocity profile moves further away from the linear profile as the temperature increases. With the non-constant material properties, we now observe that the leading order dissipation is no longer constant in the melt layer, owing to the breakdown of the linearisation

9

of the velocity profile. The dissipation term is given by

$$\Phi = \mu_0 \left(\frac{\partial v_0}{\partial X}\right)^2 + \delta \left[2\mu_0 \frac{\partial v_0}{\partial X}\frac{\partial V_1}{\partial X} + \mu_1 \left(\frac{\partial v_0}{\partial X}\right)^2\right] + O(\delta^2), \tag{26}$$

where we note that that in the leading order term both μ_0 and $\partial v_0/\partial X$ are functions of X. This should be contrasted with the dissipation for a melt layer modelled with constant material properties, which is given by

$$\Phi = \frac{1}{(X_{f0}(t))^2} + O(\delta). \tag{27}$$

Here the leading order mechanical dissipation has no spatial dependence and is proportional to the inverse square of the melt width.

With the temperature-dependent models for specific heat and viscosity we observe more mechanical heating near the sliding surface, with dissipation increasing across the layer due to the shape of the temperature profile, but decreasing globally in time due to an inverse square relation to the melt width. For the final time plotted we observe a sharp peak in the mechanical heating near $\xi = 0$ due to the considerable increase in temperature resulting from thermal runaway, Figure 3. The overall shape of the leading order dissipation profile is initially somewhat surprising, as one might expect that the dissipation should be greatest near the melt front where the viscosity is greater. However, the large velocity gradient near $\xi = 0$, which is a direct result of allowing the viscosity to depend on the temperature, more than compensates for the drop in viscosity and is in fact the driving factor in determining where the most mechanical heating takes place at leading order.
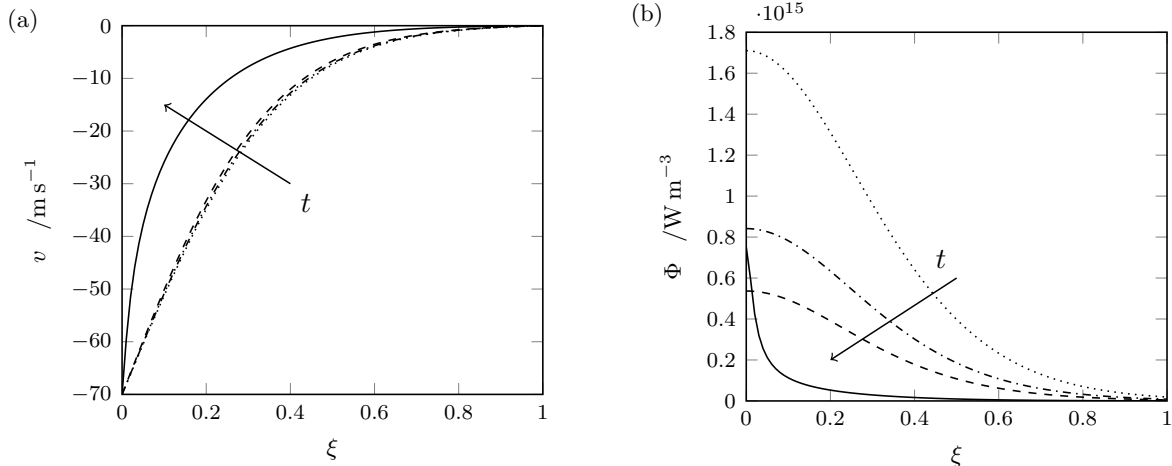

Figure 3: (a) The vertical velocity profile across the melt layer at times $t = 501, 992, 1483$ and $1974\,\text{ns}$. (b) The power density of the mechanical dissipation term as a function of $\xi = X/X_{f0}$, the front-fixed coordinate across melt layer, shown at the same times.

Figure 4 shows a comparison of the leading order temperature and power density of the Arrhenius source term for the constant material properties simulation (red dashed) and temperature-dependent

10

material properties simulation (black solid). When accounting for the temperature dependence of the specific heat and viscosity we see that the temperature profile take on a different shape across the layer due to the leading order spatial dependence in the mechanical heating. It is found that the temperature is increased adjacent to the wall and drops more rapidly across the layer when compared with previous results. Once the reaction kicks in the temperature profiles for the constant and non-constant material properties models are almost indistinguishable near the sliding surface at $\xi = 0$. By this time the power density of the reaction term has such magnitude that the differences in results owing to the modelling of the temperature-dependent specific heat and viscosity are negligible close to the reaction site.

Further from the reaction site, we see that the temperature increase in the melt layer is reduced when accounting for temperature dependence in the material properties. This is in part due to the lessened mechanical heating here, and the effect is further exaggerated by the specific heat, which increases with temperature, thus altering the shape of the temperature profile across the layer.
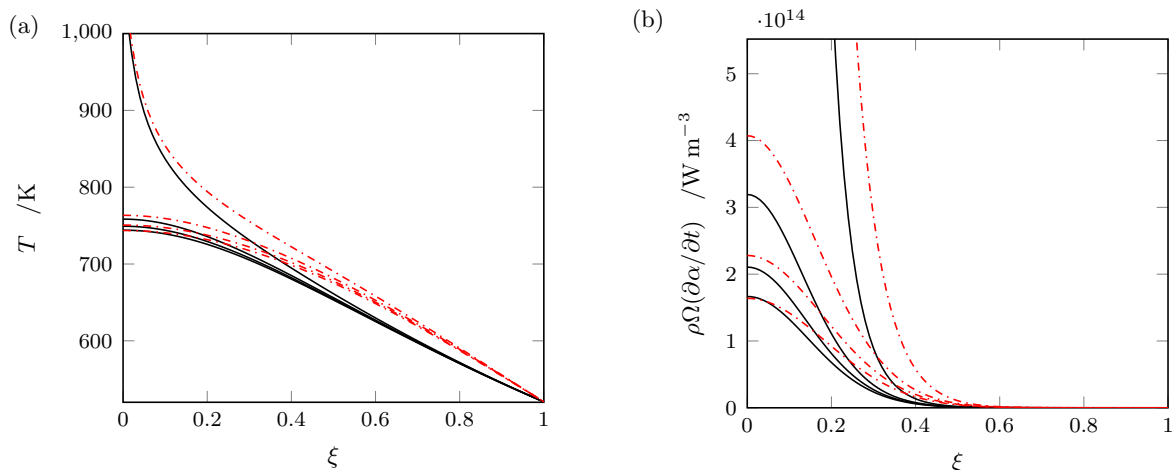

Figure 4: (a) The temperature across the melt layer, and (b) the power density of the Arrhenius source term, with constant material properties (red) and with temperature-dependent material properties (black). The plots show snapshots at approximately 25%, 50%, 75% and 100% of the time to thermal runaway. For the constant material properties simulation this corresponds to times $t = 228, 446, 664$ and $882\,\mathrm{ns}$, and for the temperature-dependent simulation the corresponding times are $t = 501, 992, 1483$ and $1974\,\mathrm{ns}$.

3.2 Two-dimensional results

Previous work has shown that when the melt layer is perturbed from one of uniform width mechanical hot spots are formed in the layer [17]. These areas of localised heating due to mechanical dissipation form either opposite or adjacent to the imposed perturbation, depending on the sign of the disturbance. It is found that perturbations which make the melt layer locally wider than the far-field width cause the formation of a mechanical hot spot on the sliding wall, whereas a hot spot is formed adjacent to the melt front in the case of perturbations which make the melt layer

locally more narrow. In both cases an accompanying "cool spot" is observed on the opposite side of the melt layer – this is an area where the local heating due to mechanical dissipation is reduced compared with the mechanical heating in the bulk of the layer.

Somewhat counterintuitively, when studying the two-dimensional we find that disturbances which widen the initial melt layer appear to be the most violent initial condition in the sense of decreasing time to runaway. Here, we choose present results for HMX with an initial melt shape $X_f(y, t_0) \sim 1 + (\delta/2)e^{-y^2}$ with $\delta = 0.8$. This particular shape was selected as in the previous work it was found to have a significant effect on the time to runaway, and thus serves as an excellent illustrative example to study when concerned with the question of whether the previously observed hot spot mechanisms persist upon inclusion of temperature-dependent material properties in the model. In such a case, an extreme localised increase in mechanical heating is observed [17]. The temperature increase due to the hot spot on the wall is sufficient to initiate a local reaction, causing the temperature to rise rapidly, see Figure 5. This has the resultant effect of causing the disturbance to grow in magnitude, causing further temperature localisation. Thus the overall time to runaway is reduced when compared with the one-dimensional case.

It is found that the introduction of temperature dependence in the specific heat and viscosity does not suppress the localisation mechanisms induced by perturbing the melt front. As found in the previous study, the imposed disturbance in the melt front causes a mechanical hot spot adjacent to the moving wall, see Figure 6. This is most clearly seen in the middle pane which shows the magnitude of the reaction source term in the melt layer – we see that the reaction is causing significant heating along the wall, owing the the increased mechanical heating near $X = 0$, but there is clearly a localised hot spot opposite the site of the disturbance in the melt front. This highly localised heating ultimately leads to a substantial temperature increase and the time to ignition is significantly decreased when compared with the corresponding one-dimensional (or, equivalently, uniform width) case.

Figure 7 (a) shows the temperature along the wall at a series of increasing times as runaway is approached. It is observed that there is a hot spot centred around $y = 0$ on the wall, resulting from the imposed melt front shape. Such a hot spot mechanisms was observed in the constant material properties model, and persists here when accounting for temperature-dependent material properties. The temperature across the layer at $y = 0$ is shown in Figure 7 at the same times. We observe a substantial temperature rise close to the wall, due to the localised increase in mechanical heating and subsequent chemical reaction.
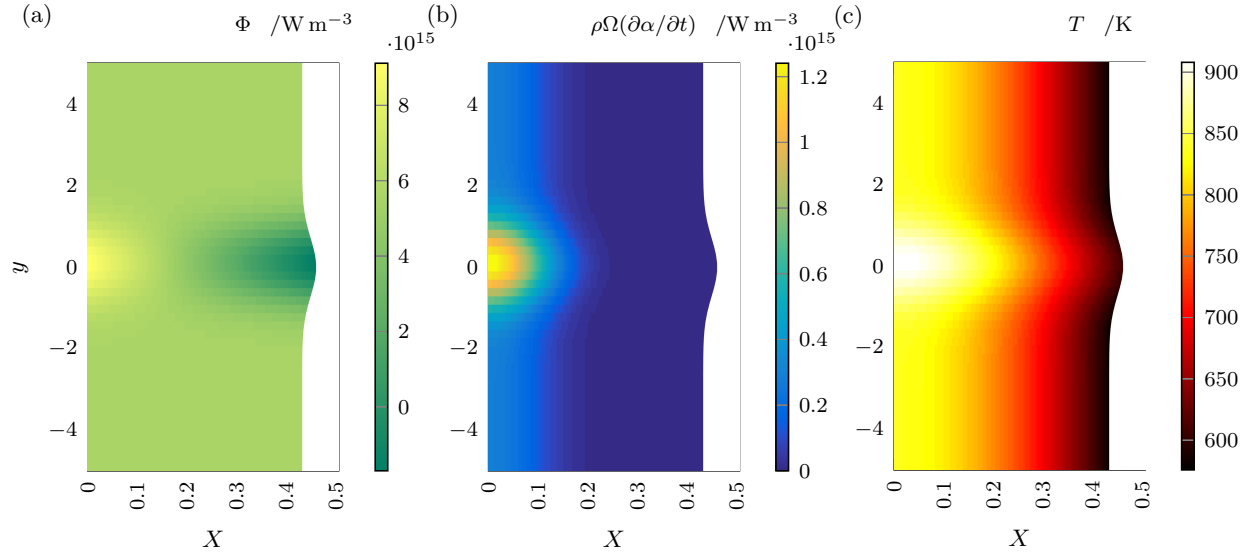
Figure 5: Snapshot of results from the constant material properties model showing: (a) Power density of mechanical dissipation source term $(\mathrm{W\,m^{-3}})$; (b) power density of Arrhenius source term $(\mathrm{W\,m^{-3}})$; and (c) dimensional temperature (K) for a sample of HMX.
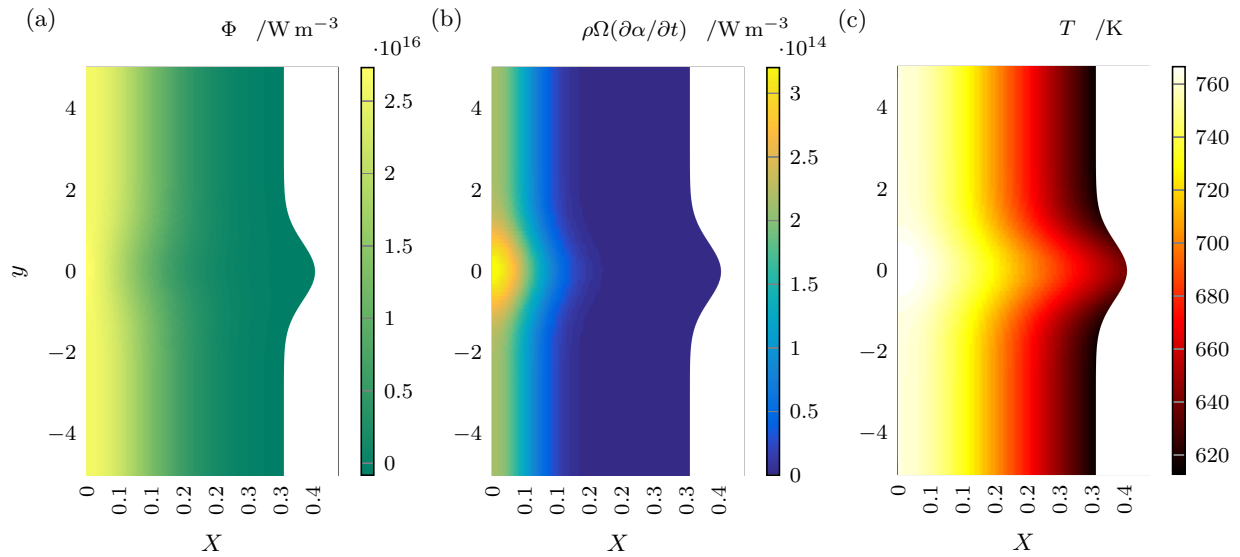

Figure 6: Snapshot of results from the temperature-dependent material properties model showing: (a) Power density of mechanical dissipation source term $(\mathrm{W\,m^{-3}})$; (b) power density of Arrhenius source term $(\mathrm{W\,m^{-3}})$; and (c) dimensional temperature (K) for a sample of HMX.
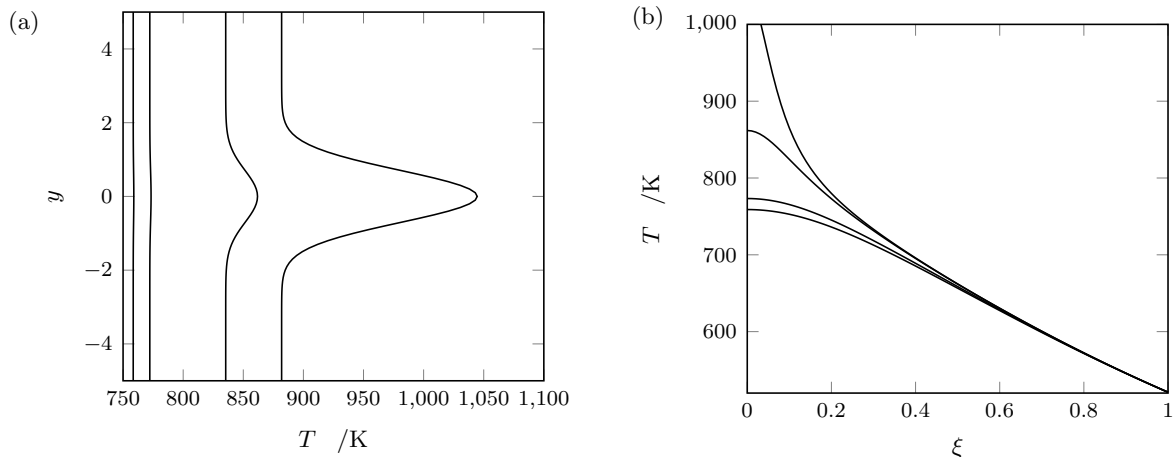
13

Figure 7: (a) The temperature along the wall $\xi = 0$, and (b) the temperature along the centreline $y = 0$ in the two-dimensional temperature-dependent material properties model at times $t = 1483, 1778, 1964$ and $1972\,\mathrm{ns}$. The solution has been computed up to $O(\delta)$.

4 Conclusions

In this study, the effects of allowing temperature-dependent material properties in a two-dimensional model for thin sheared viscous layers have been investigated. In previous work it was demonstrated that small non-uniformities in the melt front location can lead to greatly reduced runaway times due to the presence of localised hot spots. As a result, one-dimensional models of the response of explosive materials to low-speed impacts ("insults") may badly predict times to runaway. Here it has been verified that this is still the case even when accounting for temperature dependence of the material properties. That is, the predicted time to runaway may be considerably reduced when taking into account two-dimensional effects in both the constant and non-constant material properties models.

In contrast with previous work, the assumption of constant material properties has been relaxed, and the the specific heat and viscosity were allowed to vary with temperature. It was shown that the leading order (with respect to the melt front perturbation) velocity profile was no longer linear, with most of the slip being supported in the region of the melt layer adjacent to the wall. This introduced spatial dependence into the leading order mechanical dissipation term. The results suggest that the temperature dependence of material properties has the potential to be a mechanism responsible for localised reactions occurring within molten layers of explosive material, even in the absence of any other inhomogeneity.

Previously reported numerical results demonstrated that variations from a uniform width melt layer can indeed cause localised heating due to mechanical dissipation [17]. This leads to so-called hot spots in the melted explosive material. Interestingly, whilst different geometries all give rise to temperature localisation, they can have substantially different effects on the time to runaway, dependent on the hot spot location. When the melt front was perturbed, the heating mechanisms

14

observed in the constant material properties persisted in the temperature-dependent model, and the conclusions regarding melt front shape still held true.

Whilst the temperature field resulting from this model was qualitatively very similar upon comparison with earlier work which held the material properties constant, it was demonstrated that the times to ignition may change considerably when modelling the temperature dependence of the selected material properties. In order to make any concrete conclusions about the ignition times reported herein further study is needed to calibrate the models used for non-constant specific heat and viscosity. However, we remind the reader that this work is interested in the qualitative results and the results are not indented to be used for predictions of key measures such as time to onset of reaction or time to thermal runaway. As a further extension to the model, the pressure dependence of the material properties may also be studied. For example, Menikoff and Sewell [14] propose a modified form of the viscosity which increases with pressure, which may go some way to offset the drop in viscosity associated with the temperature increase across the layer.

In order to investigate any two-dimensional effects, highly idealised melt front shapes were selected. A more realistic scenario may, for example, involve choosing a shape which coincides with the grain size of the explosive material in question or with typical dimensions of grit found within the explosive. Although the grain size may be significantly larger than some of the melt thicknesses studied so far, such an approach may be more appropriate for slower wall speeds where the melt layer thickness is allowed to increase further before ignition. The solid wall used in the current formulation may also be considered as a model for a piece of high melting point grit present in the explosive sample. In any case, the heating mechanisms discussed here would still be present.

Acknowledgements

References

[1] G.T. Afanas'ev and V.K. Bobolev. *Initiation of solid explosives by impact.* Israel Program for Scientific Translations, 1971.

[2] R.A. Austin, N.R. Barton, J.E. Reaugh, and L.E. Fried. Direct numerical simualtion of shear localization and decomposition reactions in shock-loaded hmx crystal. *Journal of Applied Physics*, 117, 2015.

[3] F.P. Bowden and O.A. Gurton. Initiation of solid explosives by impact and friction: The influence of grit. *Proc. R. Soc. Lond. A*, 198(1054):337–349, 1949.

[4] F.P. Bowden and A.D. Yoffe. *Initiation and growth of explsoions in liquids and solids.* Cambridge University Press, 1952.

[5] F.P. Bowden, M.F.R. Mulcahy, R.G. Vines, and A. Yoffe. The detonation of liquid explosives by gentle impact. the effect of minute gas spaces. *Proc. R. Soc. Lond. A*, 188(1014):291–311, 1947. ISSN 0080-4630. doi: 10.1098/rspa.1947.0010.

[6] V. Boyle, R. Frey, and O. Blake. Combined pressure shear ignition of explosives. In *9th Symposium (International) on Detonation*, page 3, 1989.

[7] H.C. Chen, V.F. Nesterenko, J.C. LaSalvia, and M.A. Meyers. Shear-induced exothermic chemical reactions. *Le Journal de Physique IV*, 7(C3):C3–27, 1997.

[8] J.P. Curtis. Explosive ignition due to adiabatic shear. In *39th International Pyrotechnics Seminar*, 2013.

[9] J.K. Dienes. On reactive shear bands. *Physics Letters A*, 118(9):433–438, 1986.

[10] J.A. Dilellio and W.E. Olmstead. Shear band formation due to a thermal flux inhomogeneity. *SIAM Journal on applied mathematics*, 57(4):959–971, 1997.

[11] J.E. Field, G.M. Swallowe, and S.N. Heavens. Ignition mechanisms of explosives during mechanical deformation. *Proc. R. Soc. Lond. A*, 382(1782):231–244, 1982. ISSN 0080-4630. doi: 10.1098/rspa.1982.0099.

[12] R.B. Frey. The initiation of explosive charges by rapid shear. Technical report, DTIC Document, 1980.

[13] P.M. Howe, G. Gibbons Jr, and P.E. Webber. An experimental investigation of the role of shear in initiation of detonation by impact. Technical report, DTIC Document, 1986.

[14] R. Menikoff and T.D. Sewell. Constituent properties of hmx needed for mesoscale simulations. *Combustion theory and modelling*, 6(1):103–125, 2002.

[15] V. Krishna Mohan, V.C. Jyothi Bhasu, and J.E. Field. Role of adiabatic shear bands in initiation of explosives by drop-weight impact. In *Ninth Symposium (International) on Detonation. Office of the Chief of Naval Research, Arlington, Virginia*, pages 1276–1283, 1989.

[16] A.J. Starobin and J.K. Dienes. One-dimensional thermomechanical model for lateral melting and ignition of a thin sheared viscous layer. *Combustion Theory and Modelling*, 10(6):885–905, 2006.

[17] R. Timms and R. Purvis. A two-dimensional model for melting and ignition of a thin sheared viscous layer. In *42nd International Pyrotechnics Seminar, Grand Junction, Colorado, USA*, 2016.

[18] A.R. Ubbelohde. Part iii. (4) Mechanical and thermal processes of initiation. *Phil.Trans. of the R. Soc. Lond. A*, 241(831):280–286, 1948.